# A Simplified Analytical Model for Evaluating the Noncavitating Performance of Axial Inducers

Cristina Bramanti[*],
*ESA-ESTEC, Keplerlaan 1, Nordwijk, The Netherlands*

Angelo Cervone[†],
*Engineering Science - Osaka University, 1-3 Machikaneyama, 560-8531 Toyonaka, Osaka, Japan*

and

Luca d'Agostino[‡]
*ALTA S.p.A. - Via Gherardesca, 5 - 56121 Ospedaletto, Pisa, Italy*

**The present paper describes an analytical model for the preliminary prediction of the noncavitating flow field and performance of helical inducers. The proposed model is based on the traditional troughflow theory approximations with empirical corrections for outlet flow deviation and hydraulic losses due to inlet incidence effects and friction in the blade channels. Unlike most classical models, it allows – even if under still rather restrictive assumptions – for the prediction of the radial and circumferential flow velocity fields at the inducer exit section and for the approximate evaluation of the head coefficient as a function of the flow coefficient in terms of the static pressure rise generated by the inducer. The results are presented of the model validation by comparison with the experimental data obtained for several inducers tested in different facilities worldwide.**

## Nomenclature

| | | |
|---|---|---|
| $c$ | = | blade chord |
| $C_f$ | = | friction coefficient |
| $h_t$ | = | total enthalpy |
| $\dot{m}$ | = | mass flow rate |
| $p_{in}$ | = | inlet pressure |
| $r_T$ | = | inducer blade tip radius |
| $r_H$ | = | inducer blade hub radius |
| $s$ | = | blade solidity |
| $v$ | = | circumferential flow velocity |
| $w$ | = | axial flow velocity |
| $Z$ | = | number of blades |
| $\beta'$ | = | relative flow angle referred to the axial direction |
| $\gamma$ | = | blade angle referred to the axial direction |
| $\rho$ | = | density |
| $\sigma$ | = | cavitation number |

[*] Post-Doc Fellow, ESA Advanced Concepts Team, AIAA Member; Cristina.Bramanti@esa.int
[†] JSPS Post-Doc Fellow & Invited Foreign Researcher - Osaka University, AIAA member; angcervone@mbox.me.es.osaka-u.ac.jp
[‡] Professor, Department of Aerospace Engineering – University of Pisa, AIAA Member; luca.dagostino@ing.unipi.it

$\Phi$ = flow coefficient
$\Psi$ , $\Psi_t$ = static and total head coefficients
$\omega$ = rotational speed

## Introduction

In space rockets, turbopumps represent one of the most crucial components of all primary propulsion concepts powered by liquid propellant engines. Severe limitations are associated with the design of high power density, dynamically stable machines capable of meeting the extremely demanding pumping, suction and reliability requirements of space transportation systems (Stripling & Acosta[1], 1962). Current rocket propellant feed turbopumps often employ an inducer upstream of the centrifugal stage in order to avoid unacceptable cavitation, improve the suction performance and reduce the propellant tank pressure and weight. The main purpose of inducers is to pressurize the flow sufficiently in order to enable the main pump to operate satisfactorily. Typical inducers have fewer blades (usually 3 or 4) than centrifugal pump impellers. The main characteristic features of inducers include a low value of the working flow coefficient (typically 0.05 to 0.1), a large stagger angle (70 to 85 deg) and significantly high blade solidity. Long blades with small angle of attack provide ample time and room for the collapse of the cavitation bubbles and for the gradual exchange of energy with the flow. The resulting configuration, even though beneficial from the point of view of cavitating performance, results in highly viscous, turbulent and nonisentropic flow inside the passages.

A number of analytical models have been proposed in the past for the prediction of the inducer flow field in noncavitating and cavitating conditions. Two classical analytical models, the "ideal" and "quasi-threedimensional" models, were developed by Brennen and his collaborators for the prediction of the inducer performance in noncavitating conditions[2,3]. By introducing relatively restrictive simplifications, these models allow for the determination of the pressure coefficient as a function of the flow coefficient from consideration of the total pressure rise generated by the pump.

The analytical model presented in this paper is based on the classical throughflow theory approximations of axial turbomachinery. Unlike the classical models mentioned above, it allows – even if under still rather restrictive hypotheses – for the evaluation of radial and circumferential velocities downstream of the inducer and for the prediction of the static and total pressure coefficients as a function of the flow coefficient. The fluid is assumed to be inviscid, incompressible, axisymmetric, steady and isentropic. In accordance with the "actuator disk" approximation, the kinematic effects of the inducer blades on the flow velocity field are assumed to be uniformly concentrated at a predefined axial location, where the radial velocity is neglected (axial flow approximation), the axial component is conserved in order to satisfy the continuity equation, and the circumpherential velocity undergoes an impulsive change corresponding to the transition from the incoming flow orientation to the direction of the blade trailing edge corrected for flow deviation effects. By introducing the radial equilibrium condition, the asymptotic radial distributions of the axial and circumpherential velocity components downstream of the inducer are determined by solving a first order ordinary differential problem, whose unique integral satisfying the continuity equation fully characterizes the kinematic flow field. The pumping performance of the inducer is then obtained by application of the Euler equation with suitable loss corrections. Several approaches have been analyzed in order to evaluate the flow losses within the inducer blade passages. In particular, the empirical model proposed by Lakshminarayana[4] and a simple analytical model, developed by the authors, have been used in the following. The latter one proved to be rather predictive in the evaluation of the flow losses.

The validation of the present model has been carried out using the experimental data obtained for several different inducers[5,6,7]. The first one is a prototype of the four-bladed inducer manufactured by Avio S.p.A. and installed in the LOX turbopump of the Ariane Vulcain MK1 rocket engine. It is made in Monel, with tapered hub, constant tip radius, sharp backswept leading edges, variable blade thickness, and nonuniform axial pitch. The second inducer, called FAST2, has also been designed by Avio S.p.A. using the same criteria followed for the VINCI180 inducer. Except for having two blades, its general characteristics are qualitatively similar to those of the Ariane LOX inducer. Both of these inducers were tested in the Cavitating Pump Rotordynamic Test Facility at Alta S.p.A., Pisa, Italy. The next two inducers used for the validation are the so-called "VII" and "IX" impellers, which have been tested in the 80s at the California Institute of Technology, Pasadena, California, USA, and whose performance is extensively documented in the open literature[8]. They are helical inducers of simple geometry, with constant blade thickness, constant hub and tip radii and axially uniform pitch. The last two inducers used for the validation are two

prototypes of the LOX and LH2 inducers of the Japanese LE-7 engine (first stage of the launcher rocket H-II), tested at the Tsujimoto laboratory of the Engineering Science Department of Osaka University, Osaka, Japan.

## The Throughflow Model

Figure 1 shows the flow notations adopted in the development of the present throughflow model. As mentioned earlier, the fluid is treated as incompressible, inviscid and isentropic. Besides, at the inducer inlet and outlet (stations 1 and 2 in the figure) the flow is also assumed steady and axisymmetric with negligible radial velocity, $u \cong 0$. Then, considering the mass, angular momentum and energy balances along a streamtube between stations 1 and 2, the total enthalpy change is expressed by the well-known Euler equation:

$$h_{t2} - h_{t1} = \omega\left(r_2 v_2 - r_1 v_1\right)$$

where $\omega$ is the impeller angular speed and $v$ is the azimuthal flow velocity. By differentiating in the radial direction with:

$$h_t = h + \frac{1}{2}\left(u^2 + v^2 + w^2\right)$$

and uniform inlet flow, obtain:

$$\frac{dh_2}{dr_2} + \left(\frac{v_2}{r_2} - \omega\right)\frac{d}{dr_2}\left(r_2 v_2\right) - \frac{v_2^2}{r_2} + \frac{1}{2}\frac{dw_2^2}{dr_2} = 0$$

In the stated assumptions, the radial momentum equation in cylindrical coordinates for the outlet flow and the expression of the static enthalpy differential $dh = T\,ds + v\,dp$ give:

$$\frac{v_2^2}{r_2} = \frac{1}{\rho}\frac{dp_2}{dr_2} = \frac{dh_2}{dr_2}$$

where, from the velocity triangles of Figure 2:

$$v_2 = \omega r_2 - w_2 \tan\beta_2'$$

Elimination of $h_2$ and $v_2$ with these equations yields the following ODE for the axial velocity[12]:

$$\frac{dw_2}{dr_2} + \left[\frac{\sin^2\beta_2'}{r_2} - \frac{d}{dr_2}\ln\left(\cos\beta_2'\right)\right]w_2 - 2\omega\sin\beta_2'\cos\beta_2' = 0$$

The general solution of this equation for fully-guided flow in helical inducers where the relative flow angle is expressed by:

$$\tan\beta_2' \cong \tan\gamma_2 = \frac{r_2}{r_T}\tan\gamma_{T2}$$

as a function of the blade tip angle $\gamma_{T2}$ is:

$$w_2\left(r_2\right) = \omega r_T \frac{\left(r_2^2/r_T^2\right)\cot\gamma_{T2} + C}{r_2^2/r_T^2 + \cot^2\gamma_{T2}}$$

The integration constant $C$ is determined by the continuity equation:

$$\dot{m} = 2\pi\rho\int_{r_{H2}}^{r_T} w_2 r_2 dr_2 = \rho\Phi\omega r_T \pi r_T^2$$

as a function of the inducer flow coefficient $\Phi = \dot{m}/\pi\rho\Omega r_T^3$. With this procedure:

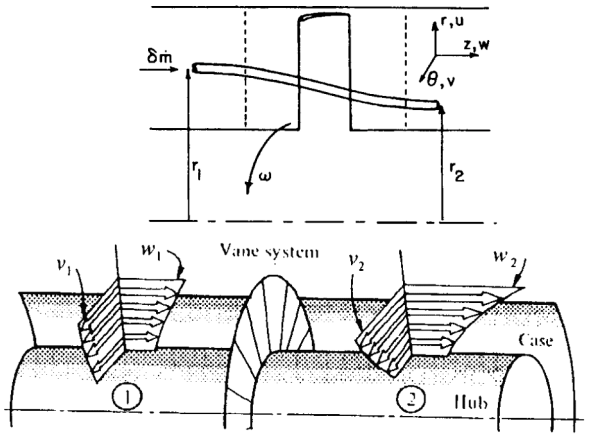


**Figure 1. Geometry of a stream tube through an axial flow turbomachine (top). Schematic of velocity components inside an axial turbomachine with the approximations of the "throughflow" model (bottom).**

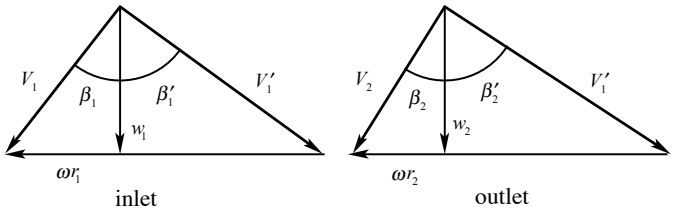


**Figure 2. Velocity triangle in the inlet (1) and outlet (2) section.**

$$\frac{w_2}{\omega r_T}=\frac{\omega r_2 - v_2}{\omega r_T \tan\beta_2'}=\cot\gamma_{T2}+\frac{\left(r_2^2/r_T^2\right)\cot\gamma_{T2}-\cot\gamma_{T2}+\Phi}{\left(r_2^2/r_T^2+\cot^2\gamma_{T2}\right)\ln K} \qquad \text{where} \qquad K=\frac{1+\cot^2\gamma_{T2}}{r_{2H}^2/r_T^2+\cot^2\gamma_{T2}}$$

Once the flow velocities have been calculated, the total and static pressure changes are readily obtained from the Euler equation:

$$p_{t2}-p_{t1}=\rho\omega r_2 v_2 \quad \Rightarrow \quad p_2-p_1=+\rho\omega r_2 v_2+\frac{1}{2}\rho\left(w_1^2-v_2^2-w_2^2\right)$$

and finally, a mean cross-sectional value of the inducer total head coefficient for comparison with the experimental results can be computed from:

$$\Psi_t=\frac{1}{r_T^2-r_{H2}^2}\int_{r_{H2}}^{r_T}\frac{p_{t2}-p_{t1}}{\rho\omega^2 r_T^2}2\pi r\,dr=\frac{1-r_{H2}^2/r_T^2+\Phi\tan\gamma_{T2}}{1-r_{H2}^2/r_T^2}\frac{1-\cot\gamma_{T2}\ln K}{\ln K}$$

as a function of the flow coefficient. As an example, Figure 3 shows the computed axial and circumferential velocities, normalized with the blade tip speed, at the exit section of the FAST2 inducer as functions of the nondimensional radial coordinate. It is possible to observe that the circumferential flow velocity $v_2$ is much larger than the axial velocity $w_2$, and has therefore to be taken into account in deriving of the total pressure rise from the measurement of the static pressure on the downstream wall of the inducer casing, as usually done in experiments.

## Evaluation of the Flow Losses

The model presented in the last Section refers to rather idealized flow conditions. In order to improve its accuracy it is therefore necessary to estimate the effects of the outlet flow deviation and hydraulic losses through the inducer by means of analytical and/or empirical equations.

The total head coefficient can be corrected to take into account the effects of the blade solidity:

$$s\left(r_2\right)=\frac{Zc\left(r_2\right)}{2\pi r_T}$$

where $Z$ is the number of blades and $c_2(r_2)$ the local blade chord, by multiplying it by the correction factor:

$$c_s\left(r_2\right)=\frac{C_L s\cos\gamma_2/\sin\left(\alpha_m+\gamma_2\right)}{2+C_L s\cos\gamma_2/2\sin\left(\alpha_m+\gamma_2\right)}$$

where $C_L$ is the lift coefficient of the blade and $\alpha_m$ is the flow angle at zero lift[10, 11]. This correction proved to be effective for typical inducer solidities ($s>1$), and has therefore been introduced in the analytical model described in the present paper.

However, even with the above correction, the model predictions were expected to significantly overestimate the performance of actual inducers because of the neglect of friction and incidence losses, as confirmed in Figure 4 with reference to the FAST2 inducer. The difference between the two curves (green triangles) is clearly indicative of the quadratic behavior typical of these losses.

Several alternative ways for evaluating the flow losses have been explored. As a first attempt, the model proposed by Lakshminarayana[4] has been investigated. In this model an "ad hoc" friction loss coefficient is empirically derived from the inducer performance data reported by various sources (NASA, MIT, TRW, etc.). Unfortunately, this correction did not provide satisfactory results when applied to the reference inducers of the present investigation,

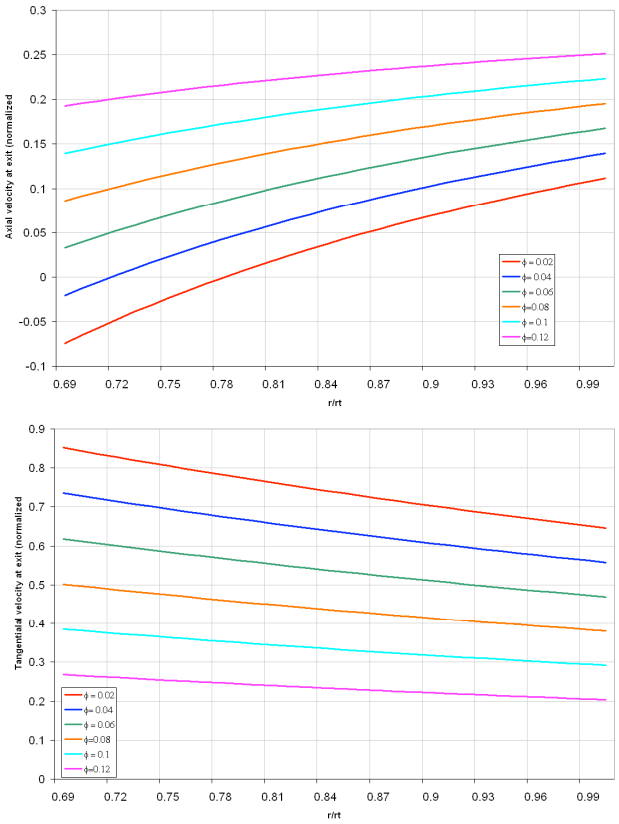


**Figure 3. Axial (top) and circumferential (bottom) flow velocities at the exit section of the FAST2 inducer, evaluated according to the "throughflow" model, as functions of the normalized radius. Velocities are normalized using the blade tip velocity, $\omega r_T$.**

probably because of their significantly different geometric characteristics with respect to those used for Lakshminarayana review. Other elementary models of performance deterioration, including slip flow corrections, leading edge flow separation, diffusion losses in blade channels and downstream mixing losses have also been investigated, but no one of them gave satisfactory results when compared to the available experimental data.

Therefore a semi-empirical model, based on a suitable combination of frictional, diffusion and incidence losses, has been developed. In this model, a first (smaller) loss contribution is represented by the flow friction along the blade channels. Since in this case the relative velocity through the blades is the relevant reference velocity, these losses have been evaluated by means of:

$$\Delta p_{L1}(r_2) = \frac{1}{2}\rho C_f \frac{c(r_2)}{2\pi r_2 / Z}\left(\frac{w_1}{\cos\gamma_1}\right)^2$$

where $C_f$ is the friction coefficient of the flow along the blade channels. As usual, integration between the hub and tip radii is required in order to obtain the overall frictional losses.

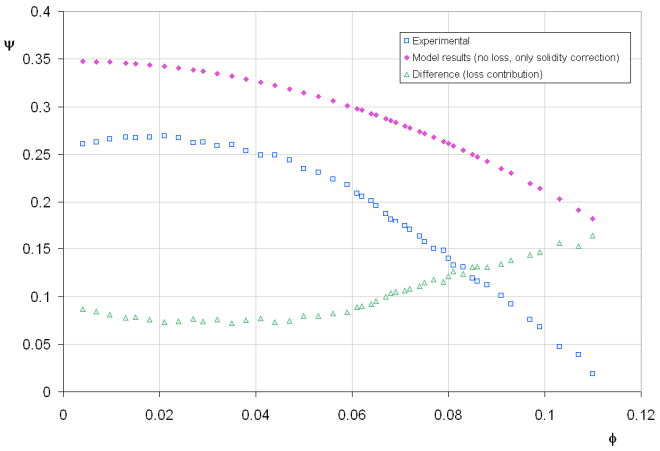


**Figure 4. Experimental performance of the FAST2 inducer (blue) compared to the model prediction with solidity correction and no flow losses (purple). The difference between the two curves is shown in green.**

A second, more significant contribution is obtained by mediating two other loss factors:

1) A "diffusion-type" loss, depending on the decrease of the relative flow velocity between the inducer inlet and the blade channels;
2) An "elbow-type" loss, generated by the deviation of the inlet flow for becoming parallel to the blade channels.

Clearly these two loss mechanisms are related. For this reason, the corresponding pressure loss has been written as:

$$\Delta p_{L2}(r_2) = \frac{1}{2}\left[\frac{1}{2}\rho V_1'^2\left(\frac{w_1/\cos\gamma_1}{\sqrt{w_1^2+\omega^2 r^2}}\right)^2 + \frac{1}{2}\rho K_{elb}(r_2) V_1'^2\right]$$

where $V_1'$ the relative flow velocity at inducer inlet and $K_{elb}$ is the loss coefficient for a duct flow in an elbow generating the same deviation as necessary in order to get the inducer inlet flow aligned with the blade channels.

The above corrections for flow deviation and hydraulic losses do not involve any adjustable factors, as required for the effective application of the proposed model to the performance prediction of newly designed inducers.

**Table 1 Geometrical and experimental characteristics of the inducers used for the validation of the model.**

| | ***MK1*** | ***FAST2*** | ***Caltech VII*** | ***Caltech IX*** | ***LE-7 LOX*** | ***LE-7 LH2*** |
|---|---|---|---|---|---|---|
| Tip radius $r_T$ (mm) | 84 | 41.1 | 50.6 | 50.6 | 74.9 | 87 |
| Inlet hub radius $r_{H1}$ (mm) | 36 | 15 | 20.24 | 20.24 | 18.7 | 25 |
| Outlet hub radius $r_{H2}$ (mm) | 58.25 | 28.3 | 20.24 | 20.24 | 38.2 | 40 |
| Inlet tip blade angle $\gamma_{T1}$ | 82.3° | 82.6° | 81° | 78° | 82.5° | 83.6° |
| Outlet tip blade angle $\gamma_{T2}$ | 72.4° | 72.5° | 81° | 78° | 81° | 78.9° |
| Number of blades | 4 | 2 | 3 | 3 | 3 | 3 |
| Solidity at tip | 3.03 | 1.54 | 1.45 | 1.75 | 1.90 | 2.11 |
| Solidity at hub | 2.5 | 1.01 | 0.62 | 0.78 | 1.00 | 1.02 |
| Distance between inducer outlet and exit pressure port | 2 diameters | 2 diameters | 2 diameters | 2 diameters | 0 diameters | 0 diameters |
| Pressure used for the reported performance (static/total) | static | static | total | total | static | static |

## Validation of the Model

As previously indicated, the proposed model has been validated against the experimental performance of six different axial inducers, which have been tested in three different facilities in the world and whose main characteristics are summarized in Table 1.

Figures 5, 6, 7 and 8 compare the noncavitating pumping characteristic of the MK1, FAST2, Caltech VII and Caltech IX inducers with the respective predictions of the present model. Good agreement has been attained for both the static head rise (MK1 and FAST2 inducers) and the total head rise (Caltech inducers). However, the results appear to be slightly less accurate in the case of Caltech inducers, probably as a consequence of their relatively low

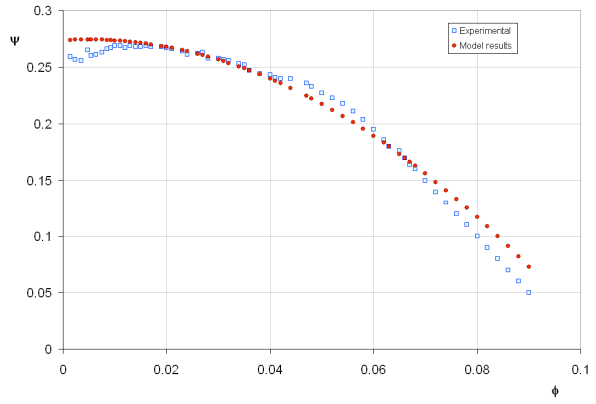


**Figure 5. Comparison between the experimental noncavitating performance of the MK1 inducer (blue) and the prediction of the analytical model (red).**

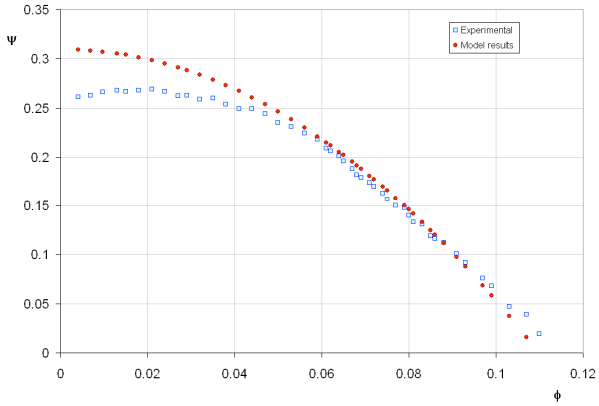


**Figure 6. Comparison between the experimental noncavitating performance of the FAST2 inducer (blue) and the prediction of the analytical model (red).**

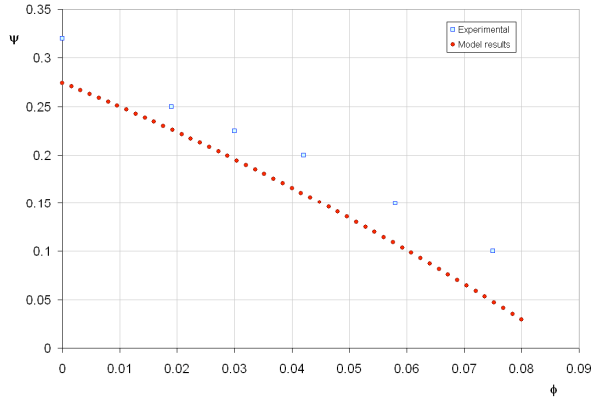


**Figure 7. Comparison between the experimental noncavitating performance of the Caltech VII inducer (blue) and the prediction of the analytical model (red).**

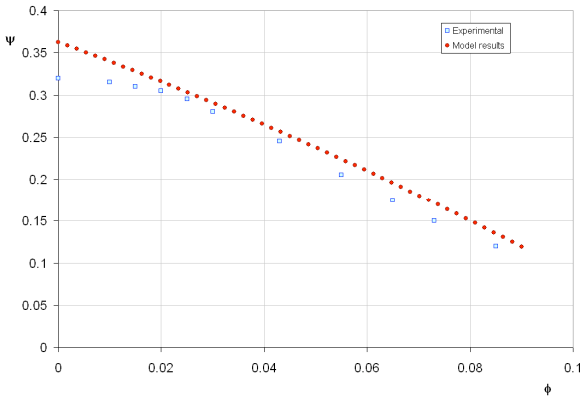


**Figure 8. Comparison between the experimental noncavitating performance of the Caltech IX inducer (blue) and the prediction of the analytical model (red).**

blade solidity (see Table 1). In particular, near the hub the solidity of these inducers is less than unity, and therefore smaller than required for accurate evaluation of flow deviation effects with the method used in the model. Furthermore, from Figures 9 and 10 it can be noted that good agreement is also obtained for the slope of the pumping characteristic, whose value is especially relevant for predicting the occurrence and nature of some of the common flow instabilities often occurring in highly-loaded inducers (in particular axial surge oscillations[9]).

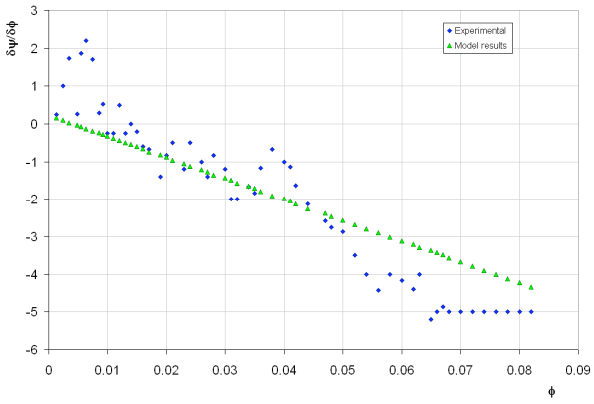


**Figure 9. Experimental performance slope of the MK1 inducer (blue) compared with the prediction of the analytical model (green).**

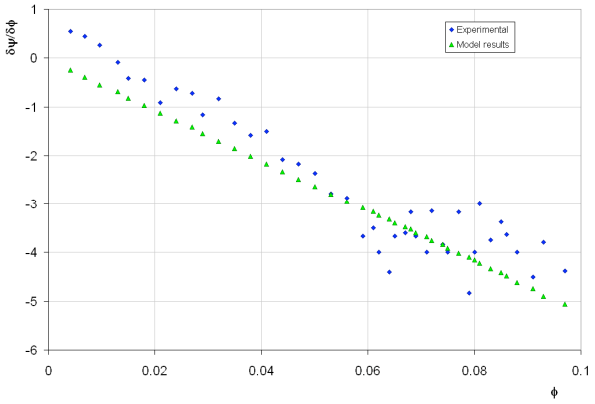


**Figure 10. Experimental performance slope of the FAST2 inducer (blue) compared with the prediction of the analytical model (green).**

Conversely, in the case of Japanese LE-7 inducers Figures 11 and 12 show that the noncavitating performance is significantly underestimated. Most likely, this situation is related to the different position of the downstream pressure tap, which in the Japanese facility is located at the blade trailing edge, while in the other cases is placed more than two diameters downstream of the inducer (see Table 1). The location of the pressure tap in the Japanese facility is clearly inconsistent with the intrinsic nature of the proposed model, whose predictions specifically refer to the fully-settled axisymmetric far-field flow downstream of the inducer. The consequent deviation of the tangential velocity profile from the radial equilibrium one introduces a systematic error in the evaluation of centrifugal effects, and therefore on the static pressure on the downstream casing of the inducer. This is confirmed by the linear behavior of the measured pumping characteristics of the Japanese inducers, which is consistent with the expected nearly uniform distribution of the axial flow velocity at the inducer trailing edge before the establishemnt of radial equilibrium conditions. The presence of the above systematic error in the evaluation of centrufugal effects is also responsible for the deterioration of the prediction of the slope of the pumping characteristic, as shown by Figures 13 and 14.

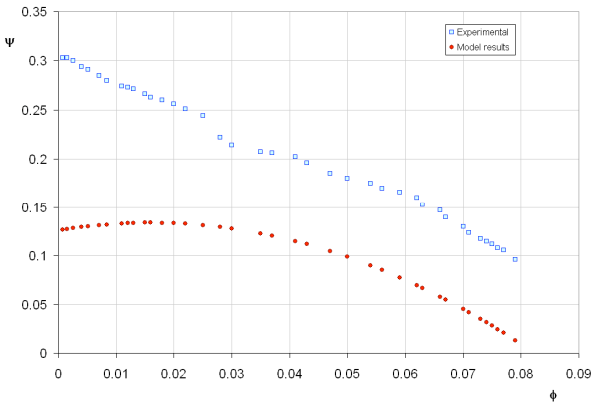


**Figure 11. Comparison between the experimental noncavitating performance of the LE-7 LOX inducer (blue) with the model predictions (red).**

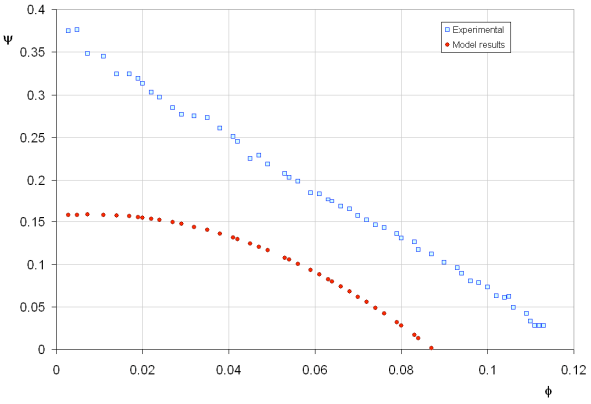


**Figure 12. Comparison between the experimental noncavitating performance of the LE-7 LH2 inducer (blue) with the model predictions (red).**

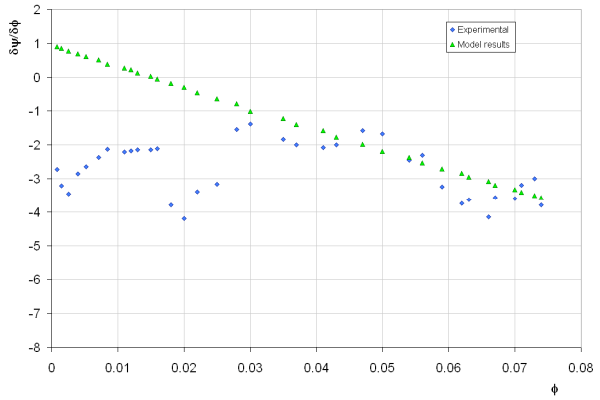


**Figure 13. Experimental slope of the pumping characteristic of the LE-7 LOX inducer (blue) compared with the model predictions (green).**

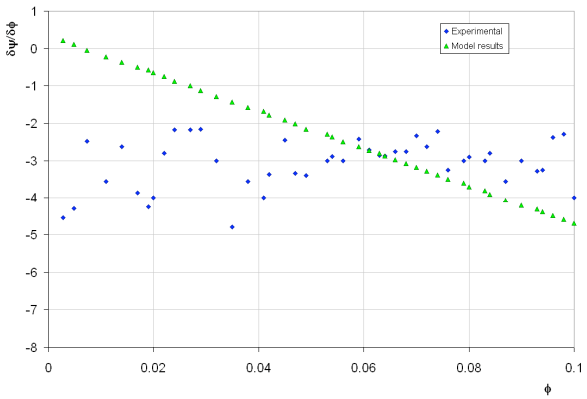


**Figure 14. Experimental slope of the pumping characteristic of the LE-7 LH2 inducer (blue) compared with the model predictions (green).**

## Conclusions

Comparison with the reference experimental results indicates that the proposed model is likely to be able of predicting with satisfactory accuracy the noncavitating performance of helical inducers. Clearly, the simplifying assumptions intrinsic in the throughflow approach and in the heuristic empirical corrections introduced in order to account for the influence of flow deviation and losses limit the realistic application of the model to inducers characterized by:

- inlet and outlet flows with negligible radial velocity, as required in the derivation of the downstream flow;
- no significant flow prerotation, and therefore, in particular, flow regimes not associated with appreciable inlet backflow;
- no downstream flow reversal, which would be incompatible with the fully-guided flow assumption at the trailing edges of the inducer blades;
- the absence of extensive flow separation at the blade leading edges, which would be inconsistent with the adopted loss model;
- relatively high values of the blade solidity and moderate values of the flow incidence on the blades, for the applicability of the deviation correction.

These conditions are usually satisfied by turbopump inducers over a relatively wide range across their nominal operating conditions. Not surprisingly, in this range the predictions of the model better agree with the reference experimental results. The systematic errors introduced by the measurement of the downstream pressure at the axial location of the blade trailing edge are likely to be responsible for the larger deviations of the model predictions from the tests data of the Japanese inducers. The available evidence suggests therefore that the proposed model may represent a useful engineering tool for preliminary estimate of the noncavitating pumping performance of helical turbopump inducers.

## Acknowledgments

The authors would like to express their gratitude to Profs. Mariano Andrenucci, Renzo Lazzeretti and Fabrizio Paganucci of the Dipartimento di Ingegneria Aerospaziale, Università di Pisa, Pisa, Italy, for their constant and friendly encouragement.

## References

[1]Stripling L.B. and Acosta A.J., "Cavitation in Turbopumps – Part 1", ASME J. Basic Eng., Vol. 84, pp. 326-338, 1962.

[2]Brennen C.E., "Hydrodynamics of Pumps", Concepts ETI, Inc. and Oxford University Press, 1994.

[3]Brennen C.E., "Cavitation and Bubble Dynamics", Oxford University Press, 1995.

[4]Lakshminarayana B., "Fluid Dynamics of Inducers - A Review", ASME Journal of Fluids Engineering, Vol. 104, pp. 411-427, Dec. 1982.

[5]Cervone A., Torre L., Fotino D., Bramanti C., d'Agostino L., "Characterization of Cavitation Instabilities in Axial Inducers by Means of High-Speed Movies", 42nd AIAA/ASME/SAE/ASEE Joint Propulsion Conference, Sacramento, USA, 2006.

[6]Cervone A., Testa R., Bramanti C., Rapposelli E. and d'Agostino L., "Thermal Effects on Cavitation Instabilities in Helical Inducers", AIAA Journal of Propulsion and Power, Vol. 21, No. 5, pp. 893-899, Sep-Oct 2005.

[7]Cervone A., Torre L., Bramanti C., Rapposelli E. and d'Agostino L., "Experimental Characterization of Cavitation Instabilities in the Avio FAST2 Inducer", 41st AIAA/ASME/SAE/ASEE Joint Propulsion Conference, Tucson, USA, 2005.

[8]Bhattacharyya A., "Internal Flows and Force Matrices in Axial Flow Inducers", Ph. D. Thesis, Report no. E249.18, California Institute of Technology, Pasadena, USA.

[9]Kawata Y., Takata T., Yasuda O., Takeuchi T., "Measurement of the Transfer Matrix of a Prototype Multi-Stage Centrifugal Pump", IMechE paper n. C346/88, 1988.

[10] Acosta, A.J., "An experimental study of cavitating inducers. Proc. Second ONR Symp. on Naval Hydrodynamics", ONR/ACR-38, 533—557, 1958.

[11] Henderson and Tucker," Performance investigation of some high speed pump inducers". R.P.E. Tech. Note 214, 1962.

[12] Saberski R.H., Acosta A.J., Hauptmann E.G., 1989, "Fluid Flow", Macmillan Publishing Co.